

Critical fields of Fe₄N/NbN ferromagnetic/superconducting multilayers

J. E. Mattson,* C. D. Potter, M. J. Conover,† C. H. Sowers, and S. D. Bader

Materials Science Division, Argonne National Laboratory, Argonne, Illinois 60439

(Received 10 May 1995; revised manuscript received 8 July 1996)

Structural, magnetic, and superconducting properties of ferromagnetic/superconducting multilayers of Fe₄N/NbN are explored for a variety of thickness combinations. The superconducting properties show that 11 Å ferromagnetic layers are sufficient to decouple the superconducting layers and to yield anisotropic behavior. The upper critical field data are well described by theory for ferromagnetic/superconducting multilayers. This analysis yields an interfacial parameter which characterizes the electron scattering at the ferromagnetic/superconducting boundary. [S0163-1829(97)05202-8]

The study of S/X multilayers where S is a superconductor and X is a nonsuperconductor has provided a fertile area in the understanding of thin-film superconductivity.¹ The superconductor may be interleaved with a variety of materials which, through the proximity effect, can alter the superconducting properties. This occurs because of both the effect of the density of states $\mathcal{N}_X(E_F)$ and the geometry of the multilayer. One example of this would be where X is an insulator yielding $\mathcal{N}_X(E_F) \sim 0$, thereby preventing coupling of the superconducting layers except through tunneling. Another example would be where X is a good metal providing a high $\mathcal{N}_X(E_F)$ and thus the possibility of proximity-induced superconductivity and consequently dimensional crossover behavior of the multilayer as a whole.²

Ferromagnetic/ X multilayers (F/X) have been no less intensely studied. When X is metallic, it is known that the conduction electrons of the intervening layer can exchange couple successive ferromagnetic layers. This coupling leads to both the giant magnetoresistance effect as well as a variety of macroscopic magnetic phenomena.³ Both the sign and strength of the coupling are crucially dependent on the choice of metal [through $\mathcal{N}_X(E_F)$] and the geometry of the layering.⁴ Much experimental work has been done in recent years to understand precisely how the Fermi surface of the metal provides this coupling.⁵

More interesting effects are likely to appear when ferromagnetic/superconducting multilayers are studied. One can view this problem from either side: an S/X multilayer with a spin-dependent $\mathcal{N}_X(E_F)$ or an F/X multilayer where exchange coupling can be affected by a temperature-dependent gap in $\mathcal{N}_X(E_F)$. Several such systems have been studied previously such as V/Fe,⁶ V/Ni,⁷ Mo/Ni,⁸ Pb/Fe,⁹ and Nb/Fe,¹⁰ with the emphasis on superconductivity.

One avenue that has been intensely pursued is Buzdin's theoretical work on ferromagnetic/superconducting systems.¹¹ Therein he predicts that the phase information of the superconducting order parameter can be transmitted across the ferromagnet, giving rise to the possibility of a π phase shift between successive superconducting layers. There have been several attempts to observe this "π phase" and one possible confirmation in the Nb/Gd system.¹²

We find that when NbN is either in the normal or superconducting state, the exchange coupling between Fe₄N layers is absent for NbN thicknesses from a few to a few hun-

dred Angstroms. Further, when the NbN is superconducting we find that very thin Fe₄N layers (~ 11 Å) are sufficient to decouple the S layers, owing to the fact that the pair-breaking effect of the F layer is substantially larger than that for normal metals. In this regime we find that the data is well described by the theoretical work of Radovic *et al.*¹³ for decoupled F/S multilayers.

Samples were prepared by reactive dc magnetron sputtering of 99.99% Nb and 99.9% Fe targets in 5–9's argon gas with a sputtering pressure of 3 mTorr of Ar and 0.5 mTorr of N₂. The sputtering rates were between 3 and 4 Å/s and the substrate-to-target distance was 9 cm. The base pressure of the sputtering system was 8×10^{-8} Torr. The sputtering conditions were similar to those used in earlier studies of NbN (Ref. 14) and Fe₄N films.¹⁵ Four series of films were made. The first series consists of single films of Fe₄N and NbN in order to establish a baseline of the single-film properties. The series of NbN films has T_c values from 14 to 16 K with widths of ≈ 0.2 K. The high-angle x-ray diffraction (XRD) spectra indicate that the NbN films are textured with a (001) orientation. Iron nitride films were found to have the structure and saturation magnetization of Fe₄N (1400 emu/cm³) and also are textured with a (001) orientation. From these results for thick films we infer that the sputtering conditions provide the proper nitrogen stoichiometry for both components.

To summarize pertinent bulk properties, Fe₄N has a cubic structure with a lattice constant $a = 3.795$ Å and is a ferromagnet with properties similar to those of bulk iron.¹⁶ NbN also has a cubic structure, but with $a = 4.38$ Å, and is a 17 K superconductor with a large upper critical field $H_{c2} \approx 25$ T and a correspondingly short Ginsburg-Landau coherence length of 50 Å.¹⁷ Note the considerable lattice mismatch of $\sim 15\%$ between the two materials.

Subsequent series were multilayers of Fe₄N/NbN in which Fe₄N was both the first layer as well as the final layer in order to insure that the pair-breaking effect of the ferromagnet is symmetric about each NbN layer. The second series has a Fe₄N layer thickness $t_F \approx 28$ Å and was grown at 400 °C on unoriented sapphire substrates. The third has $t_F \approx 17$ Å and was grown at 400 °C on MgO(100) substrates. The fourth has $t_F \approx 11$ Å and was grown at 600 °C on MgO(001) substrates. The NbN thickness t_S was varied systematically between 0 and 200 Å. More than 30 films were studied.

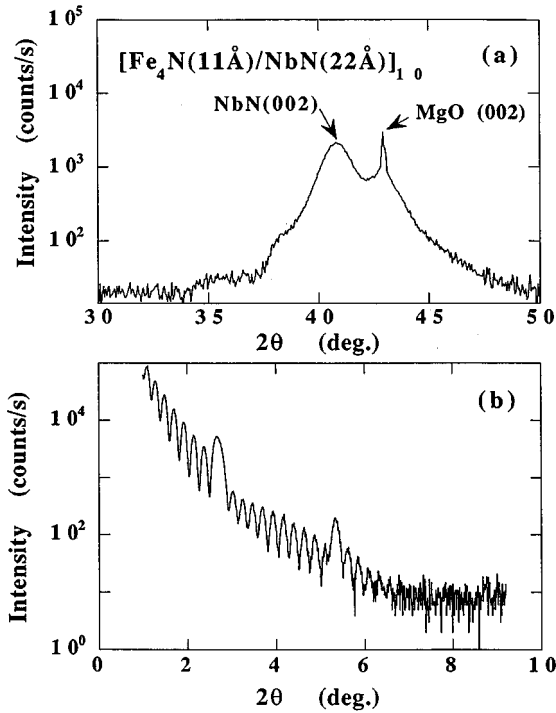


FIG. 1. XRD spectra of a $[\text{Fe}_4\text{N}(11 \text{ \AA})/\text{NbN}(22 \text{ \AA})]_{20}$ multilayer: (a) high-angle scan, (b) low-angle scan.

The structure of the multilayers was determined from both low- and high-angle XRD as shown in Fig. 1. The high-angle XRD was used to determine the growth orientation and the structural coherence length. An example of a typical high-angle XRD spectrum is shown in Fig. 1(a). This spectrum is characteristic of a multilayer for which each of the NbN layers is (001) textured but separated by a disordered Fe_4N layer. The structural coherent length, determined from the full width at half maximum of the NbN(002) Bragg peak, scales with t_S for $t_S < 80 \text{ \AA}$. The low-angle XRD shows the films to be well layered, continuous, and allows determinations of the chemical modulation period Λ to be made. Figure 1(b) shows one such low-angle XRD spectrum. A plot of Λ vs t_S was used to determine both the average t_F value (from the intercept of the plot) and to calibrate the NbN thickness (from the slope).

The magnetic properties were characterized by means of both superconducting quantum interference device magnetometry and the magneto-optic Kerr effect. Figure 2 shows a typical Kerr hysteresis loop from the 17- \AA Fe_4N series. All films in this series and the 28- \AA Fe_4N series have similar magnetic character with (i) an average Fe_4N moment of $\sim 1600 \text{ emu/cm}^3$, (ii) nearly perfect squareness in the hysteresis along the magnetic easy axis, and (iii) coercivities of order a few Oe such as shown in Fig. 2. In Fig. 3 the room-temperature squareness is plotted as M_r/M_s , the ratio of the remanent-to-saturation magnetization vs t_S for both the 17- \AA and 28- \AA Fe_4N film series. If antiferromagnetic (AF) interlayer coupling were present we would expect a characteristic reduction in the squareness and/or an increase in the saturation field. Neither is observed, thus, we conclude that AF coupling does not exist, or that the coupling is too weak ($< 10^{-3} \text{ ergs/cm}^2$) to be observed.

Films with $t_F \sim 11 \text{ \AA}$ exhibit a moment per Fe atom of

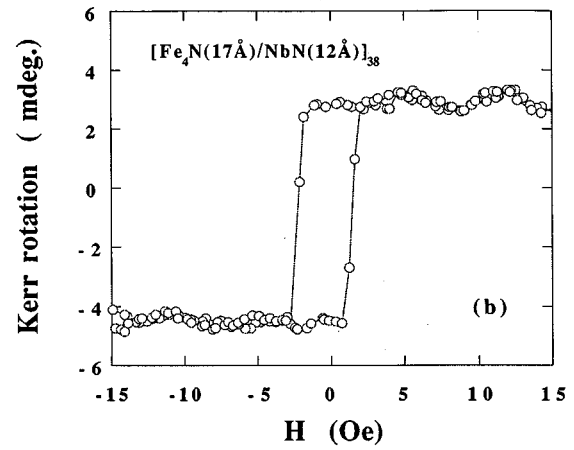


FIG. 2. Longitudinal Kerr hysteresis loop measured at room temperature for $[\text{Fe}_4\text{N}(28 \text{ \AA})/\text{NbN}(12 \text{ \AA})]_N$.

either $\sim 1/4$ or $1/2$ that of the bulk moment. The films with the larger moment resemble the thicker films with square hysteresis loops, while those with the lower moment typically exhibit a sheared hysteresis loop. This presumably arises because of disorder and thickness fluctuations in the Fe_4N layers, as seen with high-angle XRD.

The superconducting properties of the films were measured resistively using a standard four-lead dc technique with measuring currents of $10 \mu\text{A}$. Leads were attached with silver epoxy in a striped geometry. Only films with values of $t_F \sim 11 \text{ \AA}$ exhibited superconductivity, and then only for $t_S > 100 \text{ \AA}$. This is shown in Fig. 4 where T_c (defined as the midpoint of the transition in zero applied magnetic field) is plotted vs t_S . It can be seen that superconductivity is suppressed by thin Fe_4N layers for $t_S < 100 \text{ \AA}$.

The dashed line in Fig. 4 represents data taken from Ref. 18 for NbN/AlN superconducting/insulating multilayers. Comparing this to the results of our work we see that the ferromagnetic proximity effect must be responsible for the rapid drop in T_c for the $\text{Fe}_4\text{N}/\text{NbN}$ films, and that a finite-size effect alone cannot explain the T_c drop compared to the T_c value of bulk NbN. Also, in comparison to other work on F/S systems (Fig. 4) we see that the minimum t_S value for superconductivity to persist is reduced from nearly 300 \AA to almost 100 \AA in going from V or Nb to NbN.

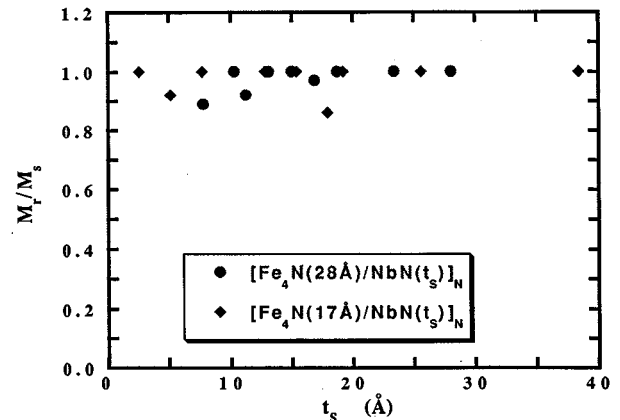


FIG. 3. Squareness vs the NbN layer thickness for $[\text{Fe}_4\text{N}(28 \text{ \AA})/\text{NbN}(x)]_N$ (circles) and $[\text{Fe}_4\text{N}(17 \text{ \AA})/\text{NbN}(x)]_N$ (diamonds).

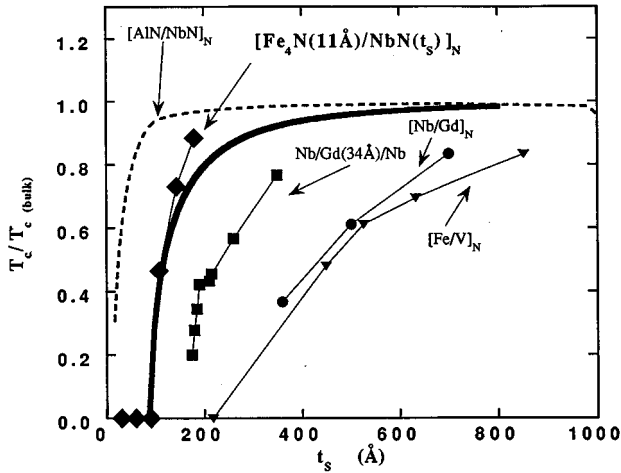


FIG. 4. T_c vs t_S for $\text{Fe}_4\text{N}/\text{NbN}$ from this work (diamonds), Fe/V (Ref. 6) (triangles), Nb/Gd (Ref. 12) sandwiches (squares) and multilayers (circles), and representative data for Nb/AlN multilayers (Ref. 18) (dashed line). The thick solid line is a fit to theory for S/F multilayers as described in the text.

Figure 5 displays the values of H_{c2} vs T in both parallel H_{\parallel} and perpendicular H_{\perp} applied fields for three films. Standard analysis of this H_{c2} data reveals that the Ginsburg-Landau coherence lengths are fairly typical for NbN , yielding about 50 to 60 Å. Notable however is that both (i) T_c is suppressed when $t_S \sim 2\xi_S$,¹⁹ as predicted by Schinz and Schwabl²⁰ for S/F multilayers, and (ii) the ratio H_{\parallel}/H_{\perp} is large which indicates that the S layers are effectively decoupled and the system is highly anisotropic. It is not possible with the available fields to determine if H_{\parallel} follows the square-root dependence indicative of two-dimensional behavior.

The suppression of superconductivity arises from the pair breaking due to the proximity to the F layers. Being an itinerant ferromagnet and having a high Curie temperature ($T_C > 300$ K), Fe_4N has a large exchange splitting. It has been suggested that superconductivity would be better preserved in the presence of an F layer with a lower T_C value such that $T_C \sim T_c$.²¹ In the present system this is not the case and the energy scale is such that $T_C(\text{Fe}_4\text{N}) \sim (20-50) T_c(\text{NbN})$. T_C values are suppressed in thin films due to finite-size effects, and reduced moments can lower T_C as well, thus the mismatch between T_C and T_c may be smaller than is estimated from the bulk T_C value. Moment reduction may explain the persistence of superconductivity observed for the samples with the thinnest (11 Å) t_F .

Since the films are in the decoupled regime we employed the theory developed by Radovic *et al.*¹³ for a fuller analysis of the H_{c2} data. This theory is appealing since, in principle, there is only one adjustable dimensionless parameter, ε , which characterizes the F/S interface. Otherwise the input to the theory is simply the bulk T_c value (17.3 K) and the bulk ξ_S value (30 Å). In practice it is necessary to allow these numbers to vary slightly. Then, given an H_{c2} value, a T_c value can be calculated through two successive root finding procedures, one of which is two dimensional.²² The theory was adapted to a standard χ^2 -fitting routine which proved quite robust.

The results of the fitting procedure are indicated by the

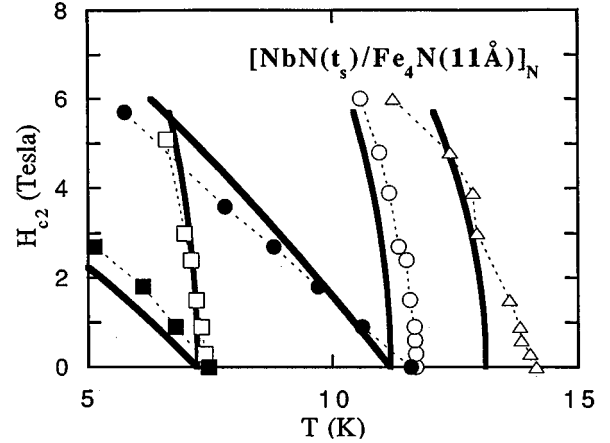


FIG. 5. H_{c2} vs T for (a) $[\text{Fe}_4\text{N}(11 \text{ \AA})/\text{NbN}(118 \text{ \AA})]_6$ (squares); (b) $[\text{Fe}_4\text{N}(11 \text{ \AA})/\text{NbN}(144 \text{ \AA})]_6$ (circles); (c) $[\text{Fe}_4\text{N}(11 \text{ \AA})/\text{NbN}(181 \text{ \AA})]_4$ (triangles). The open symbols are for H_{\perp} and the solid symbols are for H_{\parallel} . The thick solid lines are the fit to the theory for S/F multilayers as described in the text.

thick solid lines in both Figs. 4 and 5. Considering that no arbitrary scale factors have been used, the results are remarkably good. The best fit values are $\varepsilon = 3.25$ and $\xi_S = 21.9$ Å, while leaving the bulk T_c fixed at 17.3 K. We note that Radovic *et al.* used a different ε value for each superconducting thickness. We fixed ε because to do otherwise might be considered an overanalysis of a limited data set. However we note that our value for ε is similar to those found for other systems, notably V/Fe (Refs. 13 and 22) and Nb/Fe .¹⁰

The results from the fittings indicate that the influence of the F layers is quite strong and that the system is in the dirty limit. The fact that many of these F/S systems are amenable to the same dirty-limit analysis may indicate why interlayer exchange coupling may be so difficult to detect in these systems. The smearing of the Fermi surface of the S layer may destroy the static spin-density wave or magnetic quantum-well states needed for exchange coupling in multilayers. Thus, future studies might benefit from systems whose coherence lengths are even smaller than that of the present system. One likely candidate might be high- T_C materials interleaved with manganite ferromagnets.²³ Such systems have the additional advantage of having comparable (and tunable) energy scales for T_C and T_c .

In summary we have grown F/S multilayers of $\text{Fe}_4\text{N}/\text{NbN}$ via reactive sputtering. X-ray diffraction attests to the layering and (001) texturing of the films. An onset of superconductivity occurs at a NbN thickness of ~ 100 Å even for Fe_4N layers only 11 Å thick and having half the bulk moment of Fe_4N . Though this is a thinner superconducting layer than has been achieved previously in F/S multilayers, it is not sufficiently thin to simultaneously observe interlayer coupling effects. Critical field measurements are well described by the Radovic *et al.* theory for decoupled F/S multilayers, which quantify the substantial influence of the ferromagnetic proximity effect.

This work was supported by the U.S. Department of Energy, BES-Materials Sciences, under Contract No. W-31-109-ENG-38.

- *Present address: Motorola, 1301 Algonquin Road, Schaumburg, IL 60196.
- †Present address: Department of Physics, University of Illinois, Urbana, IL 61801.
- ¹V. Matijasevic and M. R. Beasley, in *Metallic Superlattices*, edited by T. Shinjo and T. Takada (Elsevier, Amsterdam, 1987), pp. 187.
- ²Ivan K. Schuller, J. Guimpel, and Y. Bruynseraede, *MRS Bull.* **15**, No. 2, 29 (1990).
- ³L. M. Falicov, Daniel T. Pierce, S. D. Bader, R. Gronsky, Kristl B. Hathaway, Herbert J. Hopster, David N. Lambeth, S. S. P. Parkin, Gary Prinz, Myron Salamon, Ivan K. Schuller, and R. H. Victora, *J. Mater. Res.* **5**, 1299 (1990).
- ⁴P. Grunberg, R. Schreiber, Y. Pang, M. B. Brodsky, and C. H. Sowers, *Phys. Rev. Lett.* **57**, 2442 (1986).
- ⁵D. Li, J. Pearson, S. D. Bader, E. Vescovo, D.-J. Huang, and P. D. Johnson (unpublished).
- ⁶H. K. Wong, B. Y. Jin, H. Q. Yang, J. B. Ketterson, and J. E. Hilliard, *J. Low Temp. Phys.* **63**, 307 (1986).
- ⁷H. Homma, C. L. S. Chun, G.-G. Zheng, and Ivan K. Schuller, *Phys. Rev. B* **33**, 3562 (1986).
- ⁸Citrad Uher, Roy Clarke, Guo-Guang Zheng, and Ivan K. Schuller, *Phys. Rev. B* **30**, 453 (1984).
- ⁹J. S. Moodera, R. Meservey, and P. M. Tedrow, *J. Magn. Magn. Mater.* **54-57**, 769 (1986).
- ¹⁰G. Verbanck, C. D. Potter, R. Schad, P. Belien, V. V. Moshchalkov, and Y. Bruynseraede, *Physica C* **235-240**, 3295 (1994); J. E. Mattson, E. E. Fullerton, C. H. Sowers, Y. Y. Huang, G. P. Felcher, and S. D. Bader, *J. Appl. Phys.* **73**, 5969 (1993).
- ¹¹A. I. Buzdin, M. Yu Kupriyanov, and B. Vujici'c, *Physica C* **185**, 2025 (1991).
- ¹²J. S. Jiang, D. Davidovic', Daniel H. Reich, and C. L. Chien, *Phys. Rev. Lett.* **74**, 314 (1994).
- ¹³Z. Radovi'c, Marko Ledvij, L. Dobrosavljevi'c-Gruji'c, A. I. Buzdin, and John R. Clem, *Phys. Rev. B* **38**, 2388 (1988).
- ¹⁴J. Talvacchio and A. I. Braginski, *IEEE Trans. Magn.* **MAG-23**, 859 (1987); J. M. Murduck, J. Vicent, I. K. Schuller, and J. B. Ketterson, *J. Appl. Phys.* **62**, 4216 (1987).
- ¹⁵K. Kijima and N. Honda, *IEEE Trans. J. Magn. Jpn.* **4**, 473 (1989).
- ¹⁶S. K. Chen, S. Jin, T. H. Tiefel, Y. F. Hsieh, E. M. Gyorgy, and D. W. Johnson, Jr., *J. Appl. Phys.* **70**, 6247 (1991).
- ¹⁷M. Ashkin, J. R. Gavaler, J. Gregg, and M. Decroux, *J. Appl. Phys.* **55**, 1044 (1984).
- ¹⁸J. M. Murduck, J. Vicent, I. K. Schuller, and J. B. Ketterson, *J. Appl. Phys.* **62**, 4216 (1987).
- ¹⁹For the remainder of the paper we use an alternate definition of coherence length, ξ_S , to be consistent with Refs. 13 and 20. The standard Ginsburg-Landau coherence length is recovered by $\xi_{GL} = \pi \xi_S / 2$.
- ²⁰H. Schinz and F. Schwabl, *J. Low Temp. Phys.* **88**, 347 (1992).
- ²¹A. I. Buzdin and M. Ledvij (private communication).
- ²²P. Koorevaar, Y. Suzuki, R. Coehoorn, and J. Aarts, *Phys. Rev. B* **49**, 441 (1994).
- ²³G. Jakob, V. V. Moshchalkov, and Y. Bruynseraede, *Appl. Phys. Lett.* **66**, 2564 (1995).